AIAA JOURNAL
Vol. 44, No. 11, November 2006

Numerical Analysis of Heaving Flexible Airfoils in a Viscous Flow

J. Pederzani* and H. Haj-Hariri†
University of Virginia, Charlottesville, Virginia 22904

DOI: 10.2514/1.21203

A numerical model for two-dimensional unsteady viscous fluid flow around flexible bodies is used to analyze the effect of chordwise flexibility on heaving airfoils. Flexible airfoils proved to be more efficient than the rigid ones. Both the output power and the input power increase in the flexible cases. The gain in efficiency is realized as a result of the output power increasing more than the input power. The density of the airfoils was shown to be a key factor in determining efficiency and power. In the parameter range analyzed, heavier airfoils are shown to generate less output power and to require proportionately less input power. Thus, heavier airfoils are more efficient than lighter airfoils. In the numerical model the bodies are represented by a distributed body force in the Navier–Stokes equations. The main advantage of this method is that the computations can be effected on a Cartesian grid, without having to fit the grid to the body surface. This approach is particularly useful when applied to the case of multiple bodies moving relative to each other, as well as flexible bodies, in which case the surface of the object changes dynamically.

Nomenclature

A	=	heave amplitude
D	=	length scale
f	=	frequency of heave
$\boldsymbol{f}$	=	body force density vector
h	=	nondimensional heave amplitude
K	=	local spring constant
k	=	nondimensional heave frequency
p	=	pressure
R	=	local radius of curvature of the membrane
Re	=	Reynolds number $=UD/\nu$
St	=	Strouhal number $=$ fA$/U$
T	=	constant pretension
t	=	time
U	=	velocity scale
u, v	=	velocity components
$\boldsymbol{v}$	=	velocity vector
x^*	=	coordinates of the "ghost" points [see Eq. (3)]
$\tilde{\boldsymbol{x}}_{l_{\text{flex}}}$	=	displacement vector of the membrane
$Y_{\max}$	=	maximum vertical displacement of the airfoil
Y_0	=	vertical displacement of the airfoil
ρ	=	density of the membrane
ν	=	viscosity of fluid
τ	=	thickness of membrane

Introduction

THE oscillation of an airfoil-like appendage, or flapping, is a common mode of propulsion for many animals. Flying animals generally use flapping to generate both thrust and lift, although many swimming species use flapping primarily to generate thrust. Recently much effort has gone into the design and construction of devices propelled by flapping, such as microair vehicles [1].

The earliest explanations of thrust generated by flapping wings date back to the early 20th century. Von Karman and Burgers [2] related the production of drag or thrust to the form of the resulting wake structures. Figure 1a shows a typical drag-producing wake behind a slowly oscillating rigid airfoil. Note that trailing edge vortices above the wake line rotate clockwise and those below rotate counterclockwise. This results in the fluid behind the airfoil moving slower than the free stream velocity, producing a momentum deficit. Conversely, Fig. 1b shows a thrust-producing wake behind a sufficiently rapidly heaving rigid airfoil. Note that the vortices have the opposite sense of rotation from the vortices in Fig. 1a, producing a momentum jet behind the airfoil.

Experimentally, Freymuth [3] demonstrated that a rigid airfoil undergoing pure pitching or pure heaving is capable of producing thrust. Jones et al. [4] used a laser Doppler velocimetry to obtain high-resolution velocity measurements in the wake of purely heaving airfoils in a water tunnel. Their experimental results confirmed the calculations of Triantafyllou et al. [5], which identified the Strouhal number as an important parameter for the generation of thrust.

Garrick [6] extended computations of Theodorsen [7] to determine the thrust produced by an airfoil undergoing small-amplitude heaving oscillations in an inviscid, incompressible fluid. He concluded that all pure heaving motions generate thrust and that thrust is proportional to the square of the frequency. He also noted that propulsive efficiency drops off asymptotically from 1.0 at low frequencies to 0.5 at high frequencies. The thrust and the input power both go to zero at low frequencies, thus giving rise to an efficiency of one. The results are based on linearized theory and ignore any viscous flow contributions; nevertheless, they indicate the fundamental need to balance total thrust production with propulsion efficiency.

Several authors have developed and applied unsteady lifting-line methods to model flapping flight. The models excluded the unsteady effects of the vortex wake. Phlips et al. [8] modeled the wake using both a near wake component consisting of a vortex sheet and a far wake component consisting of discrete vortices. Self-induced convection of the wake was still neglected. Furthermore the method was limited to low frequency flapping in inviscid flows. In general, lifting-line methods have proven useful in understanding the qualitatively effects of the wake structures on the aerodynamics. But the inherent assumptions in the method, namely small-amplitude motions, high aspect ratios, and low flapping frequency, make the method overly restrictive [9].

Unsteady panel methods have also been used to model flapping flight. Such methods rely on the distribution of inviscid singularities on the aerodynamic surfaces (e.g., source or vortex panels) to model flow over an airfoil or body. The wake is modeled either with a series

Received 16 November 2005; revision received 19 June 2006; accepted for publication 23 June 2006.

*Graduate Student, Mechanical and Aerospace Engineering Department, P.O. Box 400746; pederzani@virginia.edu.

†Professor, Mechanical and Aerospace Engineering Department, P.O. Box 400746; haj-hariri@virginia.edu.

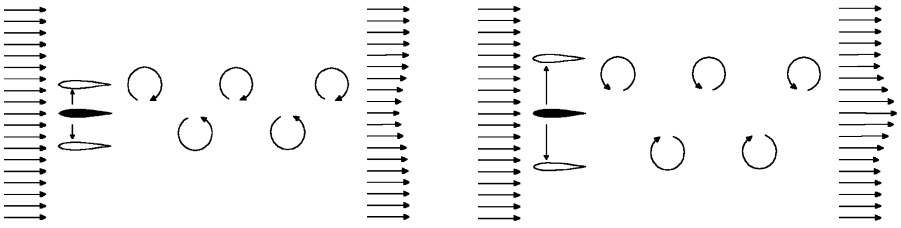

a) Drag producing wake behind a slowly oscillating airfoil.

b) Thrust producing wake behind a rapidly oscillating airfoil.

Fig. 1 Wake behind airfoils.

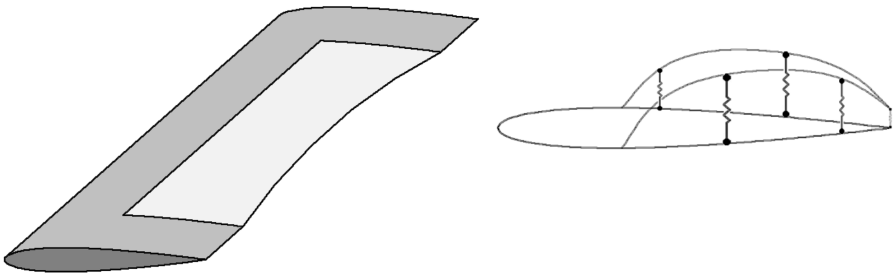

a) **b)**

Fig. 2 Flexible wing a) and airfoil b).

of panels trailing behind the body, or with discrete vortex elements. Various unsteady forms of the Kutta condition are employed to determine the rate at which vorticity is shed into the wake. Also the methods allow for self-convection of the wake. However, they are still based on ideal flows. Jones and Platzer [10] and Jones et al. [4] developed an inviscid model to determine the forces on a two-dimensional airfoil undergoing simultaneous pitching and heaving. The vorticity being shed into the wake was modeled as an extra panel, the length, orientation, and vortex strength of which was determined as part of the solution. They were able to reproduce the wake structure and momentum profiles for small-amplitude pitching and heaving airfoils. At small amplitudes the viscous effects are not as pronounced in the topology of the vorticity field, and the inviscid assumption is more justified.

Hall and Hall [11] developed a vortex lattice method to determine the optimal circulation distribution for a prescribed combination of lift and thrust. The method consisted of finding time-dependent circulation distribution that minimizes induced losses without concern for the details of the mechanics of the flapping motion. This method was later extended by Hall et al. [12] to include viscous drag component determined from quasisteady analysis at each spanwise wing section. The model explicitly assumes light wing loading and low reduced frequency.

Daube et al. [13] developed a viscous numerical model to investigate dynamic stall due to pitching of an airfoil at low to moderate frequencies and Reynolds numbers ranging from 3,000–10,000. The model was only used to test low frequency oscillations. No thrust was produced in their model, nor did it exhibit leading edge.

Liu et al. [14] created a three-dimensional Navier–Stokes solver. They were able to successfully reproduce the major three-dimensional features of the fluid, although their model predicted larger than expected lift coefficients. The most notable flow features observed were the generation of a large leading-edge vortex on both the up- and down strokes. This vortex remained attached during pronation and supination before being shed at the beginning of the subsequent stroke. Also, the vortex was shown to be much stronger near the wing tip, creating a low pressure core that sucks fluid

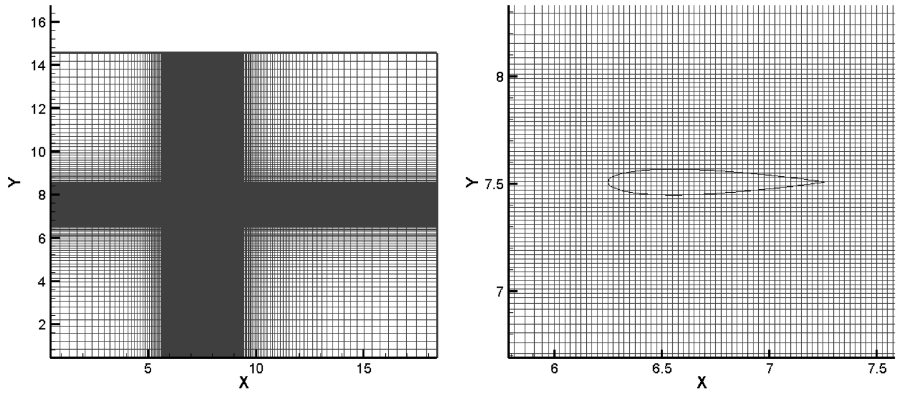

a) Grid used for the CFD calculations.

b) Airfoil and portion of the grid used for the CFD calculations, every other line is shown

Fig. 3 Computational grid.

spanwise from the base of the wing to the wing tip. Such three-dimensional effects might be important in stabilizing the vortex to enhance the effects of dynamic stall.

Wang [15] correlated the optimum frequency for heaving airfoils to the time-scale of vortex shedding for impulsively started airfoils. For sufficiently large local angles of attack, an impulsively started airfoil will generate net thrust for a short period until a leading-edge vortex is shed.

More recently Lewin and Haj-Hariri [16] developed a numerical model for two-dimensional flow around an airfoil undergoing prescribed heaving motions in a viscous flow. They showed that for a given Strouhal number the maximum efficiency occurs at an intermediate heaving frequency. This is in contrast to ideal flow models, in which efficiency increases monotonically as frequency decreases. The separation of the leading-edge vortices at low heaving frequencies leads to diminished thrust and efficiency. At high frequencies, the efficiency decreases similarly to the prediction of inviscid theory.

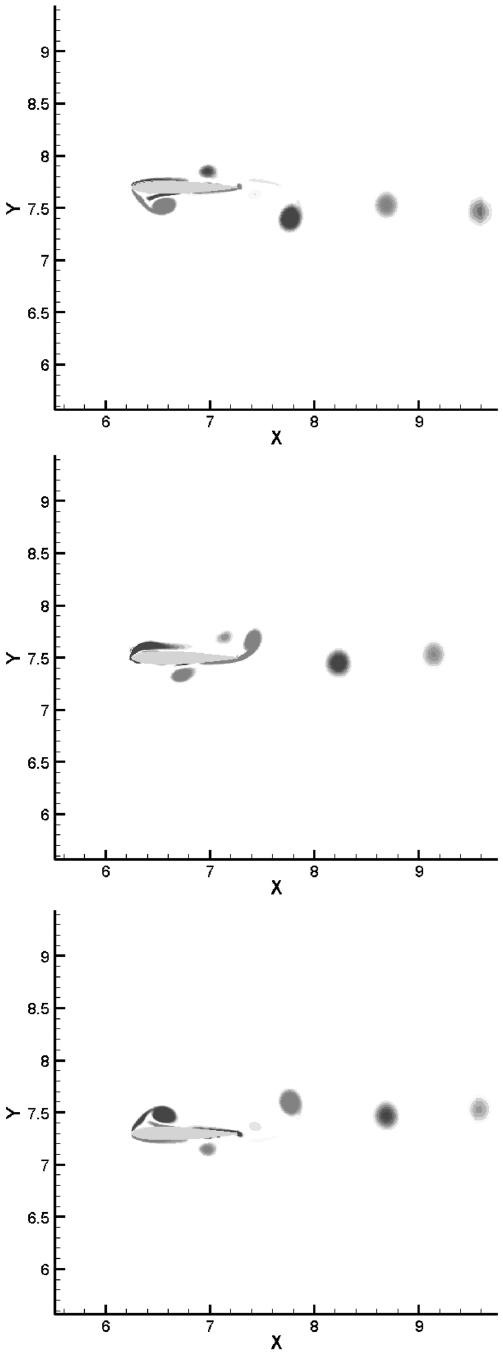

Fig. 4 Vorticity field generated by a rigid airfoil heaving at $kh = 0.8$ and $k = 4.0$.

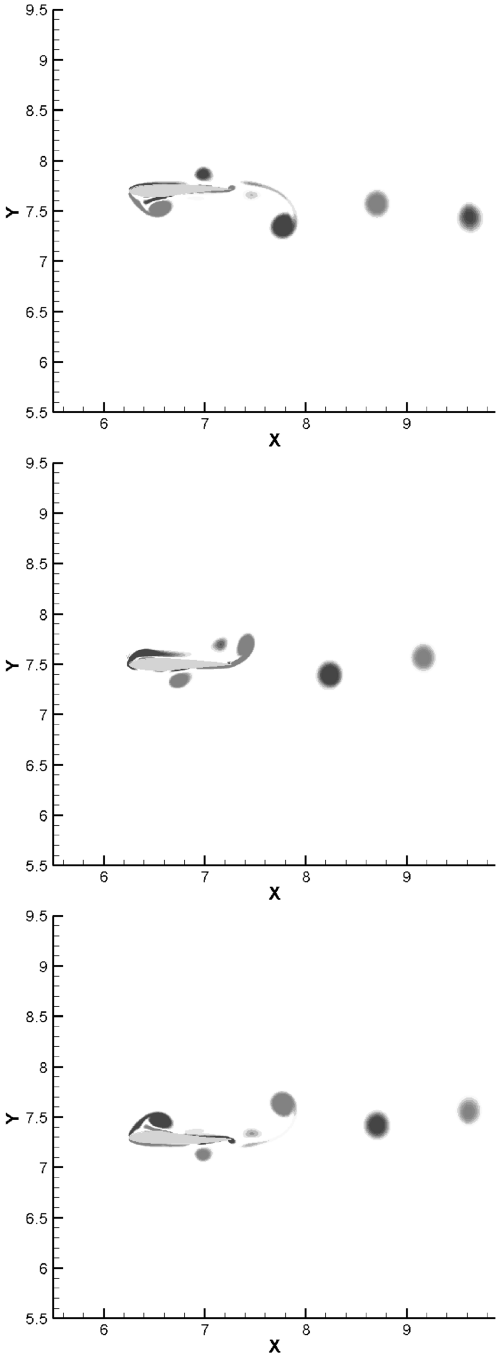

Fig. 5 Vorticity field generated by a flexible airfoil heaving at $kh = 0.8$ and $k = 4.0$.

All animals that use flapping as a mode of propulsion, manifest in their wings or fins some form of flexibility, be it passive, active, or both. Passive flexibility is in the case that the shape of the wing fin is modified only as a reaction to the flow, and the animal has no control on it. On the contrary in the case of active flexibility, it is the animal that controls the deformation of the wing or fin through the use of its muscles. Wu [17,18] analyzed the problem of optimum shape for a flexible plate in motion in an inviscid flow, and showed it possible to obtain a propulsive efficiency higher than that of a rigid plate. Calculations by Katz and Weihs [19,20] showed that an airfoil with passive chordwise flexibility oscillating in an inviscid flow has an increased propulsive efficiency, but a sightly decreased overall thrust.

More recently, Prempraneerach et al. [21] conducted an experimental analysis to show the effects of chordwise flexibility

on the thrust and efficiency of a flapping foil. Foils of different flexibilities were all observed to give rise to an increase in the propulsive efficiency. In some cases both the propulsive efficiency and the thrust increased.

The purpose of this work is to use a computational model, recently developed by the authors [22], to shed light on the role of chordwise flexibility of a heaving airfoil in a viscous flow.

Problem Definition

The model developed is used to simulate a two-dimensional incompressible viscous flow around a heaving flexible airfoil. The governing equations are the continuity and Navier–Stokes equations

$$\nabla \cdot \boldsymbol{v} = 0 \tag{1}$$

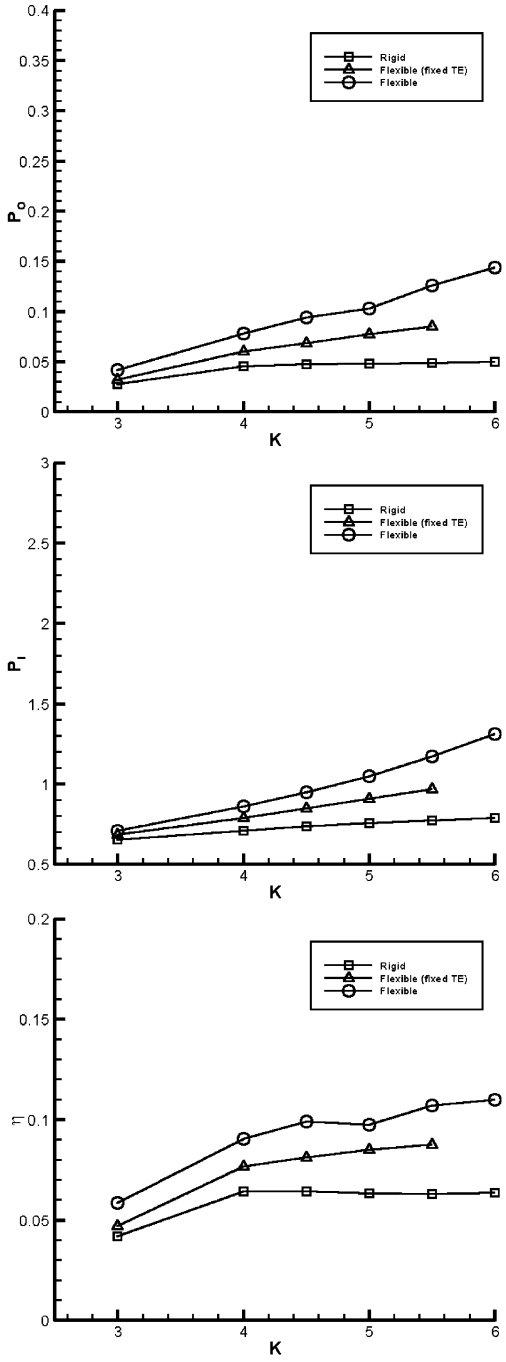

Fig. 6 Average output and input power and efficiency for the three different airfoils for $kh = 0.8$.

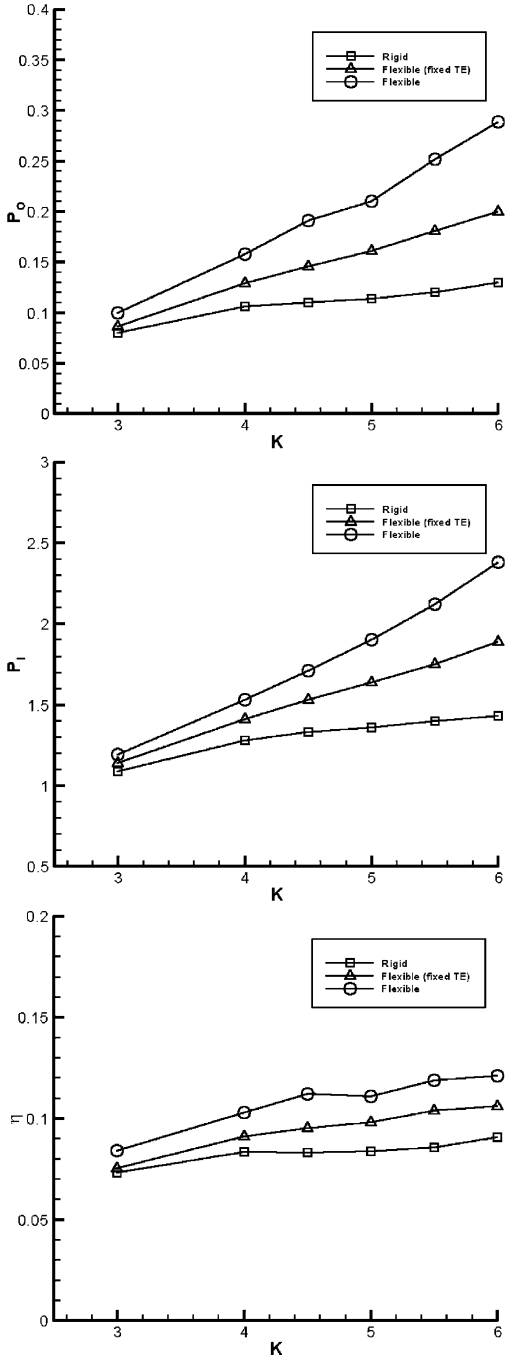

Fig. 7 Average output and input power and efficiency for the three different airfoils for $kh = 1.0$.

$$\frac{\partial \boldsymbol{v}}{\partial t} = -\boldsymbol{v} \cdot \nabla \boldsymbol{v} + \frac{1}{Re}\nabla^2 \boldsymbol{v} - \nabla p + \boldsymbol{f} \tag{2}$$

The equations are written in dimensionless form. Here, p is scaled with ρU^2 and $\boldsymbol{f}$ is scaled with $\rho U^2/D$.

The heaving motion of the airfoil is an arbitrary function of time. In this work the base mode of oscillation for the airfoil is represented as a sinusoidal function of time:

$$Y_0 = Y_{\max} \sin(2\pi f t)$$

Introducing k and h

$$k = \frac{2\pi f c}{U}, \qquad h = \frac{Y_{\max}}{c}$$

the nondimensional position and the heave velocity of the airfoil are given, respectively, as

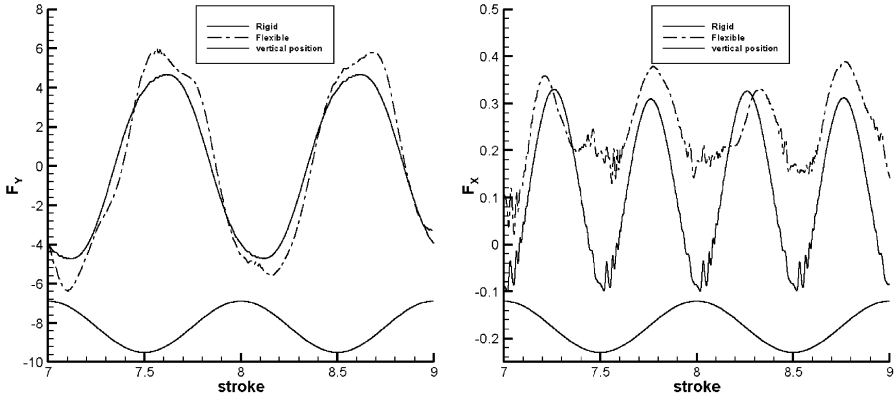

a) Vertical force **b) Horizontal force**

Fig. 8 Nondimesional forces acting on the rigid and flexible airfoils for $kh = 1.0$ and $k = 5.5$.

$$\bar{Y}_0 = h\sin(kt), \qquad \bar{V}_0 = kh\cos(kt)$$

The parameter kh, which differs from the Strouhal number by a factor of π, is the nondimensional maximum heave velocity, and is an important factor in determining thrust or drag production.

We consider a rigid wing, from which a portion has been cut out, covered with a very thin and flexible material, latex for example, as shown in Fig. 2a. Our interest is focused on the middle plane section of the wing, Fig. 2b. The flexible part of the airfoil is modeled as two thin membranes, one for the upper surface of the airfoil and one for the lower, joined at the trailing edge. The leading edge and the first 40% of the airfoil are going to be considered rigid, whereas the remaining portion, including the trailing edge is going to be modeled as flexible. Because membranes are not able to resist bending and because they are fixed only at two points and not at the trailing edge, which is free to move, the structure is not able to self-sustain itself in two dimensions (although it clearly does in three dimensions). Therefore a distribution of springs, as shown in Fig. 2b, which connect the membrane to ghost points on a rigid skeleton, is used in order to simulate the out-plane tension that is actually present in the three-dimensional wing, and that is not reproducible in two dimensions. The ghost points move with the velocity of the rigid portion of the airfoil and essentially mimic the effect of the rigid frame of the wing as shown in Fig. 2a. The model for the membrane assumes only normal displacements. The equation used to represent such displacements is

$$\rho\tau\left(n_x\frac{\partial^2\tilde{y}_{l_{\text{flex}}}}{\partial t^2} - n_y\frac{\partial^2\tilde{x}_{l_{\text{flex}}}}{\partial t^2}\right) = \frac{T}{R} - p - K[n_y(\tilde{y}_{l_{\text{flex}}} - y_l^*) + n_x(\tilde{x}_{l_{\text{flex}}} - x_l^*)] \tag{3}$$

In the equations the only forcing coming from the fluid p, whereas the shear stress, due to its small value, is neglected. The membrane has no extensional stiffness. Also the membrane stretch, being negligible, is not taken into account.

Numerical Implementation

The approach developed is a mixed Eulerian–Lagrangian one. The body surface is represented using Lagrangian points $(\tilde{x}_l, l = 1, \ldots, L)$. The governing equations for fluid flow, Eqs. (1) and (2), are solved everywhere, including the cells which are occupied by the solid body, using a Eulerian approach. The presence of the solid body is accounted for by adding a force field to the momentum equation in those cells that are fully or partially occupied by the solid phase. The magnitude and direction of this body force density is determined at every time step of the computation by requiring the value of the velocity in those cells to match the prescribed, or actual, velocity of the solid body. This is achieved with the aid of a volume-fraction field which determines what fraction of each computational cell in the Cartesian grid is occupied by the solid

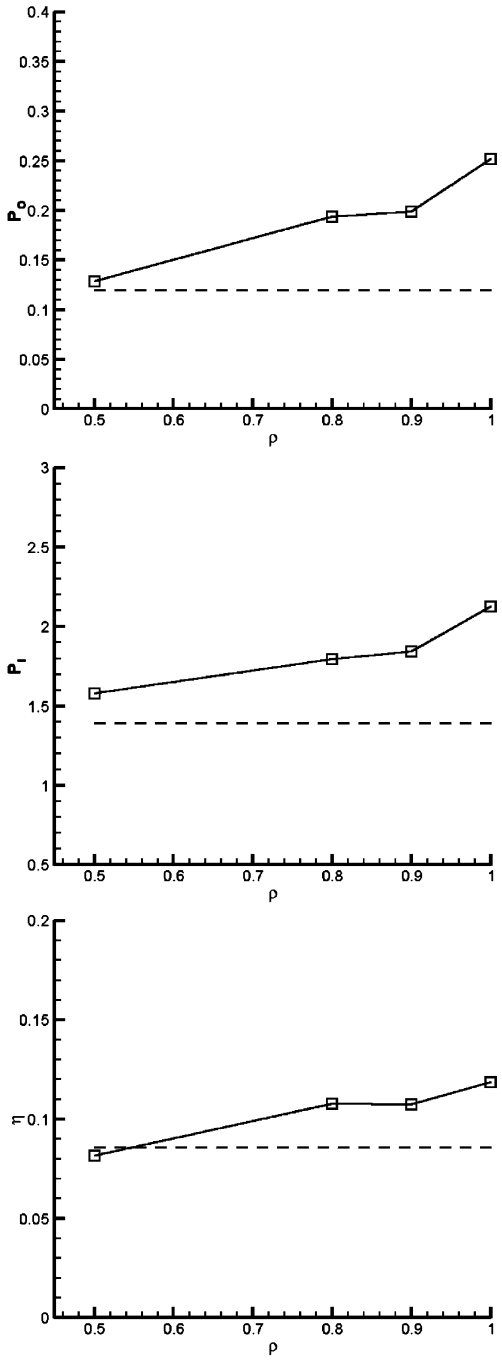

Fig. 9 Average output and input power and efficiency for airfoils of different densities heaving at $kh = 1.0$ and $k = 5.5$.

phase. In cells where the solid volume fraction is unity, the velocity is set exactly equal to that of the body, and in those where the volume fraction is between zero and one, the velocity is only adjusted partially, in proportion to the volume fraction. Fluid cells are not affected in that step of the computation. The details of the model are presented in Pederzani and Haj-Hariri [22].

Fluid Solver

Equations (1) and (2) are solved on a nonuniform Cartesian mesh, as shown in Fig. 3, using a finite-difference formulation with a staggered grid approach [23].

In the staggered grid, within cell (i, j), the pressure and volume-fraction fields are assigned to the cell center, whereas the horizontal and vertical velocity components are assigned to the midpoints of the right and top edge of the cell, respectively. The grid size used is 224×352 with $\Delta x = 0.0125$ and $\Delta y = 0.01$ (in the uniform part of the grid). Three-point centered differencing is used to approximate the spatial derivatives, and forward differencing is used for the time derivative. In order for stability of this scheme the time step, dt has to be smaller than $1/Re$. The time step used in this simulation is smaller than the required limit so as to resolve the motion of the airfoil adequately.

Boundary conditions are imposed using ghost cells at the outer limits of the computational domain. For the velocity field, the inflow is prescribed to be $u = 1$ and $v = 0$ corresponding to a uniform longitudinal flow. On the lateral boundaries the conditions are free slip and impermeability; that is, $\partial u/\partial y = 0$ and $v = 0$, respectively. The free slip condition prevents the viscous boundary layers from growing on those walls. At the outflow, the velocity components are assumed to possess zero normal gradients: $\partial u/\partial x = 0$ and $\partial v/\partial y = 0$. For the pressure, in the transverse direction homogeneous Neumann conditions are applied at the lateral walls, $\partial p/\partial y = 0$, whereas in the longitudinal direction $\partial p/\partial x = 0$ is imposed at the inlet and $p = 0$ at the outlet.

Membrane Solver

The membrane Eq. (3) is solved with a Newmark scheme [24]. Consider the following second order differential equation:

$$y''(t) = \phi(t, y) \tag{4}$$

The Newmark scheme consists of the following finite-difference scheme for Eq. (4)

$$y^{n+1} - 2y^n + y^{n-1} = \Delta t^2[\beta\phi^{n+1} + (\tfrac{1}{2} - 2\beta + \gamma)\phi^n + (\tfrac{1}{2} + \beta - \gamma)\phi^{n-1}] \tag{5}$$

The scheme is second order accurate for $\gamma = \frac{1}{2}$, whereas it is just first order accurate for $\gamma \neq \frac{1}{2}$. For $\beta = 0$ the scheme is explicit. Moreover for $\gamma = \frac{1}{2}$ and $\beta = 0$ it coincides with the leapfrog scheme. It can be shown that for $\beta = 1/4$ and $\gamma = 1/2$ the Newmark scheme (5) is unconditionally stable.

Results

To understand the role of flexibility in flapping airfoil, the numerical model developed [22], was used to analyze several cases.

The Reynolds number used in all simulations is $Re = 500$, which is typical of insect flight. Several heaving motions were simulated for three different types of airfoil. The first airfoil was rigid and used as reference. The other two were flexible; one had a fixed trailing edge (relative to the rigid forepiece) whereas the other allowed the trailing edge to move. The fixing or moving of the trailing edge was achieved by connecting the junction point of the two membranes to the rigid frame with a spring. In the first case the spring was so stiff that no displacement of the trailing edge was allowed, in the second case the stiffness of the spring was reduced in order to allow the trailing edge to move.

All three types of airfoil were simulated at different frequencies of heave for two different values of kh: 0.8 and 1.0. In Figs. 4 and 5 the flow fields generated by a heaving rigid and flexible airfoil are shown. The flow field generated by the flexible airfoil hardly differs from the one generated by the rigid airfoil. The vortex pattern is the same in both cases. Although the flexible airfoil alters the flow field only slightly, with respect to the rigid one, these modifications are significant enough to change the forces acting on the airfoil substantially. This is the main contribution of the current article.

It was found that the flexible airfoils were more efficient than the rigid one for all the different heave parameters as shown in Figs. 6 and 7. The efficiency increase is the result of the output power increasing proportionally more than the input power. This is in contrast with previous studies [17–20]. In fact, although these studies predicted an increase in efficiency in the case of flexible plates and airfoils compared to the rigid ones, their input and output power were both lower than a rigid foil. This is due to the fact that previous models not only assume an inviscid flow, but also the plates and airfoils in the previous studies were massless.

Mass (and therefore inertia) play an important role in a fluid-structure interaction problem. This is seen easily when the vertical and horizontal forces acting on the airfoil are analyzed. The comparison of the vertical force of the flexible case against that for the rigid case, shows how differences arise mainly at some particular station of the flap. The vertical force, both for the flexible case and rigid case, present the same oscillatory behavior, though the maximum, which is reached shortly after the beginning of a stroke [see Fig. 8a], is higher in the flexible case. This is due to the mass of the membrane. During the beginning of the stroke the membrane is pulled and, therefore, accelerated by the rigid frame. When the rigid part starts decelerating the membrane, due to its mass, does not do so as quickly and at the end of the stroke it has a non zero velocity in the direction opposite to that of the following stroke. Therefore, more power is needed at the beginning of each stroke to snap the membrane back. The motion of the airfoil can be summarized as follows: at the beginning of each stroke power has to be put in the airfoil to reverse the tail, then the tail starts to catch up with the rigid portion and eventually passes it until it reaches the end of the stroke and reverses again.

The comparison of the horizontal force, Fig. 8b, of the flexible case against the one of the rigid case, shows how, due to the snapping, the strength of the vortices that are shed is higher in the flexible case, leading to the generation of more thrust.

For the flexible airfoil with fixed trailing edge, the overshoot is smaller, thus each flaps requires less input power and generates less output power than the case of the fully flexible airfoil, but more than the rigid case.

To analyze the role of the mass of the membrane, heaving airfoils with different densities were simulated heaving for a particular kh and k. The range of densities analyzed is small, but of practical interest, and such that the natural frequency of the structure is significantly higher than the heaving frequency. And so the motion remains dominated by stiffness effects. Figure 9 shows how lighter airfoils require less input power and produce less output power. This is due to the fact that a lighter membrane requires less input power in order to be snapped. The snapping motion is less strong than in the rigid case and generates less output power. Lighter airfoils are less efficient as the output power decreases proportionately more then input power.

The lightest membrane that was simulated shows a value of efficiency that is lower than the one for the rigid case. This is the only case in our simulations and is not in line with the results of our study. Prempraneerach et al. [21], though, in their experimental work also found one case, out of the many analyzed, in which a flexible airfoil was less efficient than a rigid one.

Conclusions

A numerical study shows chordwise flexibility in heaving airfoils to improve efficiency and increase output power in most cases. The simulations were conducted for two different types of flexible airfoils, one with a fixed trailing edge and one with a loose trailing edge. The airfoil with the loose trailing edge was shown to be the

more efficient of the two. It was also shown that, for certain parameters, heavier airfoils are capable of generating more thrust than lighter ones, and are also more efficient.

Acknowledgments

The authors acknowledge the support (financial and otherwise) provided by James Batterson of NASA Langley Research Center under Grant No. NAG 1-01120. Jean-Noel Pederzani also gratefully acknowledges the financial support of the Farrar fellowship.

References

[1] Ashley, S., "Palm-Size Spy Planes," *Mechanical Engineering*, Vol. 120, No. 2, 1998, pp. 74–78.

[2] Von Karman, T., and Burgers, J. M., *Aerodynamic Theory*, Vol. 2, Springer, Berlin, 1935.

[3] Freymuth, P., "Propulsive Vortical Signature of Plunging and Pitching Airfoils," *AIAA Journal*, Vol. 26, No. 7, 1988, pp. 881–883.

[4] Jones, K. D., Dohring, C. M., and Platzer, M. F., "Wake Structures Behind Plunging Airfoils: A Comparison of Numerical and Experimental Results," AIAA Paper 96-0078, Jan. 1996.

[5] Triantafyllou, G. S., Triantafyllou, M. S., and Grosenbaugh, M. A., "Optimal Thrust Development in Oscillating Foils with Application to Fish Propulsion," *Journal of Fluids and Structures*, Vol. 7, 1993, pp. 205–224.

[6] Garrick, I. E., "Propulsion of a Flapping and Oscillating Airfoil," NACA, Tech. Rept. 567, 1936.

[7] Theodorsen, T., "General Theory of Aerodynamic Instability and the Mechanism Of Flutter," NACA, Tech. Rept. 496, 1935.

[8] Phlips, P. J., East, R. A., and Pratt, N. H., "An Unsteady Lifting Line Theory of Flapping Wings with Application to the Forward Flight of Birds," *Journal of Fluid Mechanics*, Vol. 112, 1981, pp. 97–125.

[9] Smith, M. J. C., Wilkin, P. J., and Williams, M. H., "The Advantages of an Unsteady Panel Method in Modeling the Aerodynamic Forces on Rigid Flapping Wings," *Journal of Experimental Biology*, Vol. 199, No. 5, 1996, pp. 1073–1083.

[10] Jones, K. D., and Platzer, M. F., "Numerical Computation of Flapping-Wing Propulsion and Power Extraction," AIAA Paper 97-0826, Jan. 1997.

[11] Hall, K. C., and Hall, S. R., "Minimum Induced Power Requirements for Flapping Flight," *Journal of Fluid Mechanics*, Vol. 323, 1996, pp. 285–315.

[12] Hall, K. C., Pigott, S. A., and Hall, S. R., "Power Requirements for Large-Amplitude Flapping Flight," *Journal of Aircraft*, Vol. 35, No. 3, 1998, pp. 352–361.

[13] Daube, O., Ta Phuoc, L., Dulieu, A., Coutanceau, M., Ohmi, K., and Texier, A., "Numerical Simulation and Hydrodynamic Visualization of Transient Viscous Flow Around an Oscillating Aerofoil," *International Journal for Numerical Methods in Fluids*, Vol. 9, No. 8, 1989, pp. 891–920.

[14] Liu, H., Ellington, C. P., Kawachi, K., van den Berg, C., and Willmott, A. P., "A Computational Fluid Dynamics Study of Hawkmoth Hovering," *Journal of Experimental Biology*, Vol. 201, No. 4, 1998, pp. 461–477.

[15] Wang, Z. J., "Vortex Shedding and Frequency Selection in Flapping Flight," *Journal of Fluid Mechanics*, Vol. 410, 2000, pp. 323–341.

[16] Lewin, G. C., and Haj-Hariri, H., "Modelling Thrust Generation of a Two-Dimensional Heaving Airfoil in a Viscous Flow," *Journal of Fluid Mechanics*, Vol. 492, 2003, pp. 339–362.

[17] Wu, T. Y.-T., "Hydromechanics of Swimming Propulsion, Part 1: Swimming of a Two-Dimensional Flexible Plate at Variable Forward Speeds in an Inviscid Fluid," *Journal of Fluid Mechanics*, Vol. 46, No. 2, 1971, pp. 337–355.

[18] Wu, T. Y.-T., "Hydromechanics of Swimming Propulsion, Part 2: Some Optimum Shape Problems," *Journal of Fluid Mechanics*, Vol. 46, No. 3, 1971, pp. 521.

[19] Katz, J., and Weihs, D., "Hydrodynamic Propulsion by Large Amplitude Oscillation of an Airfoil with Chordwise Flexibility," *Journal of Fluid Mechanics*, Vol. 88, No. 3, 1978, pp. 485–497.

[20] Katz, J., and Weihs, D., "Large Amplitude Unsteady Motion of a Flexible Slender Propulsor," *Journal of Fluid Mechanics*, Vol. 90, No. 4, 1979, pp. 713–723.

[21] Prempraneerach, P., Hover, F. S., and Triantafyllou, M. S., "The Effect of Chordwise Flexibility in the Thrust and Efficiency of a Flapping Foil," *Proceedings of the Thirteenth International Symposium on Unmanned Untethered Submersible Technology: Proceedings of the Special Session on Bio-Engineering Research Related to Autonomous Underwater Vehicles*, Autonomous Undersea Systems Institute, Lee, New Hampshire, 2003.

[22] Pederzani, J., and Haj-Hariri, H., "A Numerical Method for the Analysis of Flexible Bodies in Unsteady Viscous Flows," *International Journal for Numerical Methods in Engineering* (to be published).

[23] Harlow, W. W., and Welch, J. E., "Numerical Calculation of Time-Dependent Viscous Incompressible Flow of Fluid with Free Surface," *Physics of Fluids*, Vol. 46, 1965, pp. 2182–2189.

[24] Nobile, F., "Fluid-Structure Interaction Models in Hemodynamics," Master's Thesis, Technical University of Milan, 1998, in Italian.

C. Pierre
Associate Editor